47th AIAA Aerospace Sciences Meeting Including The New Horizons Forum and Aerospace Exposition
5 - 8 January 2009, Orlando, Florida

AIAA 2009-1333

Partition Design and Optimization for High-Order Spectral Volume Schemes

Rob Harris[1]
CFD Research Corporation, Huntsville, AL 35805

Z. J. Wang[2]
Department of Aerospace Engineering, Iowa State University, Ames, IA 50011

An analysis of the accuracy and stability properties of the spectral volume (SV) method, with applicability to very high-order accurate simulations, is presented. In the SV method, each simplex grid cell is called a spectral volume (SV), and the SV is further partitioned into polygonal (2D), or polyhedral (3D) control volumes (CVs) to support high-order data reconstructions. In general, the partitioning of an SV into CVs is not uniquely defined, and thus it is of great importance to select a partition which yields favorable stability properties, and results in an interpolation polynomial of high quality. Here we present a new approach to efficiently locate stable partitions by means of constrained minimization. This is motivated by the fact that, at present, an exhaustive search approach to SV partition design would be prohibitively costly and thus not feasible. Once stable partitions are located, a high quality interpolation polynomial is then assured by subsequently minimizing the dissipation and dispersion errors of the stable partitions. Results are presented which demonstrate the potential of this method for producing stable and highly accurate partitions of arbitrary order. In particular, a new 4^{th}-order partition is presented which has improved accuracy and stability properties over previously used partitions, and a new stable 5^{th}-order partition is introduced.

I. Introduction

The spectral volume (SV) method is a recently developed finite volume method for hyperbolic conservation laws on unstructured grids.[1-7] The SV method belongs to a general class of Godunov-type finite volume method[8-9], which has been under development for several decades, and is considered to be the current state-of-the-art for the numerical solution of hyperbolic conservation laws. For a more detailed review of the literature on the Godunov-type method, refer to Wang[1], and the references therein. Many of the most popular numerical methods, such as the k-exact finite volume[10-11], the essentially non-oscillatory (ENO)[12-13], and weighted ENO[14] methods are also Godunov-type methods. A thorough review and comparison of these methods can be found in Wang.[15] The SV method is also closely related to the discontinuous Galerkin (DG)[16-20] method, a popular finite-element method for conservation laws. Both the SV and DG methods employ multiple degrees of freedom within a single element, but the SV method avoids the volume integral required in the DG method. Each simplex in the SV method utilizes a "structured" set of sub-cells, or control volumes (CVs), to support a polynomial reconstruction for the conserved variables, and a nodal set to support a polynomial reconstruction for the flux vector. For a more thorough comparison of the SV and DG methods, refer to Wang.[1,15]

The partitioning of an SV into CVs has been one of the greatest challenges in the implementation of the SV method since its inception. This partitioning defines the reconstruction stencil, and thus plays a vital role in determining the accuracy and stability properties of the scheme. Early on, several researchers focused on using the Lebesgue constant as a means to design accurate SV partitions. In particular, the work of Wang[2], Liu[5], and Chen[21,22] is of relevance. While this criteria may be used to find partitions with lower error bounds, it does not guarantee that a particular scheme will be more or less accurate, and it offers no information about the stability of the scheme. A positive step towards addressing the issue of stability was given by Van den Abeele et al.[23-25]. In this work, some previously used SV partitions were found to be

[1]Project Engineer, Aeromechanics Dept., 215 Wynn Drive, reh@cfdrc.com, AIAA Member.
[2]Professor of Aerospace Engineering, 2271 Howe Hall, zjw@iastate.edu, Associate Fellow of AIAA.

weakly unstable, and several new stable partitions were proposed. It was also shown that the new partitions had lower dissipation and dispersion errors than some previously used partitions despite having larger Lebesgue constants. This showed that although the Lebesgue constant should be small to ensure a lower upper bound on the error, it need not be minimal for a scheme to possess superior accuracy.

This paper is organized as follows. In Section 2, we review the basic formulation of the SV method. After that, the framework for stability analysis of the SV method is described in detail in Section 3. Next, the methodology for partition design and optimization is outlined in Section 4. Numerical results are then given in Section 5, including stability and accuracy studies for new impoved 4th and 5th-order partitions. Finally, conclusions are summarized in Section 6.

II. Review of the spectral volume method

Consider the multidimensional conservation law

$$\frac{\partial Q}{\partial t}+\frac{\partial f(Q)}{\partial x}+\frac{\partial g(Q)}{\partial y}+\frac{\partial h(Q)}{\partial z}=0, \tag{1}$$

on domain $\Omega \times [0,T]$ and $\Omega \subset R^3$ with the initial condition

$$Q(x,y,z,0)=Q_0(x,y,z), \tag{2}$$

and appropriate boundary conditions on $\partial\Omega$. In (1), x, y, and z are the Cartesian coordinates and $(x,y,z) \in \Omega$, $t \in [0,T]$ denotes time, Q is the vector of conserved variables, and f, g and h are the fluxes in the x, y and z directions, respectively. Domain Ω is discretized into I non-overlapping triangular (2D), or tetrahedral (3D) cells. In the SV method, the simplex grid cells are called SVs, denoted S_i, which are further partitioned into CVs, denoted $C_{i,j}$, which depend on the degree of the polynomial reconstruction. Volume-averaged conserved variables on the CVs are then used to reconstruct a high-order polynomial inside the SV. To represent the solution as a polynomial of degree m, we need N pieces of independent information, or degrees of freedom (DOFs). Where N is calculated as follows:

$$N=\frac{(m+1)(m+2)\cdots(m+d)}{d!}, \tag{3}$$

where d is the spatial dimension of the problem. The DOFs in the SV method are the volume-averaged conserved variables at the N CVs. Define the CV-averaged conserved variable for $C_{i,j}$ as

$$\overline{Q}_{i,j}=\frac{1}{V_{i,j}}\int_{C_{i,j}} Q dV, \quad j=1,\ldots,N, \quad i=1,\ldots,I, \tag{4}$$

where $V_{i,j}$ is the volume of $C_{i,j}$. Given the CV-averaged conserved variables for all CVs in S_i, a polynomial $p_i(x,y,z) \in P^m$ (the space of polynomials of at most degree m) can be reconstructed such that it is a $(m+1)^{\text{th}}$ order accurate approximation to $Q(x,y,z)$ inside S_i.

$$p_i(x,y,z)=Q(x,y,z)+O\left(h^{m+1}\right), \quad (x,y,z)\in S_i, \quad i=1,\ldots,I, \tag{5}$$

where h is the maximum edge length of all the CVs. This reconstruction can be solved analytically by satisfying the following condition:

$$\frac{1}{V_{i,j}}\int_{C_{i,j}} p_i(x,y,z)dV=\overline{Q}_{i,j}, \quad j=1,\ldots..,N. \tag{6}$$

This polynomial $p_i(x,y,z)$ is the $(m+1)^{th}$ order approximation we are looking for as long as the solution $Q(x,y,z)$ is smooth in the region covered by S_i. The reconstruction can be expressed more conveniently as

$$p_i(x,y,z)=\sum_{j=1}^{N} L_j(x,y,z)\overline{Q}_{i,j}, \tag{7}$$

where $L_j(x,y,z) \in P^m$ are the shape functions which satisfy

$$\frac{1}{V_{i,j}}\int_{C_{i,j}} L_n(x,y,z)dV=\delta_{jn}. \tag{8}$$

Integrating (1) in $C_{i,j}$, we obtain

$$\frac{d\overline{Q}_{i,j}}{dt}+\frac{1}{V_{i,j}}\sum_{r=1}^{K}\int_{A_r}\left(\vec{F}\cdot\vec{n}\right)dA=0, \qquad j=1,\ldots,N, \qquad i=1,\ldots,I, \tag{9}$$

where $\vec{F}=(f,g,h)$, A_r represents the r^{th} face of $C_{i,j}$, $\vec{n}$ is the outward unit normal vector of A_r, and K is the number of faces in $C_{i,j}$. More details of this, including representative plots of the shape functions can be found in Wang[2]. The integral in (9) can be computed using Gauss quadrature, or using the quadrature-free

approach outlined in Harris et al.[7] For time integration, we use either the 2nd- or 3rd-order SSP Runge-Kutta scheme from Gottlieb et al.[26] Some recent accomplishments in the development and application of the SV method can be found in Harris and Wang[27-28] and the references therein.

It was shown in Wang and Liu[2] that the so-called Lebesgue constant computed as

$$\left\|\Gamma_{\Pi}\right\| = \max_{\xi,\eta} \sum_{j=1}^{N} \left|L_j(\xi,\eta)\right|, \tag{10}$$

gives a simple method of bounding the interpolation polynomial for the SV method. Thus the smaller the Lebesgue constant $\left\|\Gamma_{\Pi}\right\|$, the better the interpolation polynomial in terms of error bounds. However, although this criteria can be helpful in finding accurate SV partitions, it carries no information about the stability properties of the resulting scheme, and is thus a necessary but not sufficient tool for designing SV partitions.

III. Formulation for stability analysis

The wave propagation properties associated with a particular SV partition and Riemann flux carry information about both the accuracy and stability of the numerical scheme. Recent work by Van den Abeele et al.[23-25] has utilized the so-called Fourier footprint to facilitate the design of stable SV partitions with favorable wave propagation properties. A similar analysis is employed here.

Consider the 2D linear advection equation

$$\frac{\partial Q}{\partial t} + \nabla \cdot (\vec{a} Q) = 0, \tag{11}$$

with periodic boundary conditions, where $\vec{a} = a(\cos\psi, \sin\psi)$ is the wave propagation velocity, and ψ is the wave propagation direction. The initial solution is taken to be a harmonic plane wave

$$Q(x, y, 0) = e^{Ik(x\cos\theta + y\sin\theta)}, \tag{12}$$

with wave number k, orientation angle θ, and I is the square root of -1. The SV method is then applied to (11) on a grid comprised entirely of equilateral triangles. The simplest unit which produces the entire grid when periodically repeated, commonly referred to as the generating pattern (GP), is shown in Figure 1.

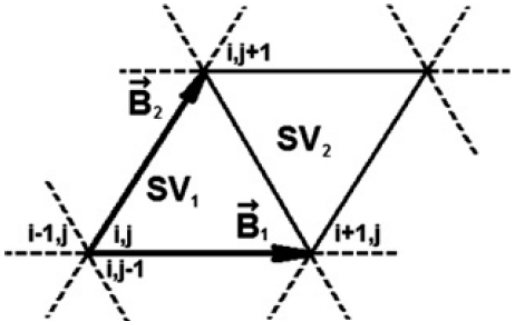

Figure 1. Generating pattern for the grid (taken from Van den Abeele and Lacor[24]).

The GP is completely defined by the vectors $\vec{B}_1$ and $\vec{B}_2$. On the boundary between two SVs, the following Riemann flux is employed

$$\hat{F}(Q_L, Q_R) = \frac{1}{2}\left(\vec{a}\cdot\vec{n} + \varphi\left|\vec{a}\cdot\vec{n}\right|\right)Q_L + \frac{1}{2}\left(\vec{a}\cdot\vec{n} - \varphi\left|\vec{a}\cdot\vec{n}\right|\right)Q_R, \tag{13}$$

where Q_L is the solution due to the SV to the left of the face, Q_R is the solution due to the SV to the right of the face, and φ is an upwinding parameter, where $\varphi = 0$ gives rise to a central flux, and $\varphi = 1$ results in a simple upwind flux. After applying the SV method to (11), we obtain

$$\sum_{n=1}^{2N}\left[\frac{V'\Delta B}{a}U_{m,n}\frac{d\overline{Q}_{i,j;n}}{dt} + M^{0}_{m,n}\overline{Q}_{i,j;n} + M^{-1}_{m,n}\overline{Q}_{i-1,j;n} + M^{+1}_{m,n}\overline{Q}_{i+1,j;n} + N^{-1}_{m,n}\overline{Q}_{i,j-1;n} + N^{+1}_{m,n}\overline{Q}_{i,j+1;n}\right] = 0, \tag{14}$$

where ΔB is the magnitude of $\vec{B}_1$, a is the magnitude of $\vec{a}$, V' is the volume of an SV nondimensionalized by ΔB^2, the index m varies from 1 to $2N$, and the indices i and j denote a particular GP. The variables $\overline{Q}_{i,j;n}$ for $n = 1$ to N are the CV-averages corresponding to the first SV in the GP (SV_1), while the variables for $n = N + 1$ to $2N$ are the CV-averages corresponding to the second SV in the GP (SV_2), and the matrices $U_{m,n}$, $M^{0}_{m,n}$, $M^{-1}_{m,n}$, $M^{+1}_{m,n}$, $N^{-1}_{m,n}$, and $N^{+1}_{m,n}$ are functions of the wave propagation direction and their definitions can be found in Van den Abeele and Lacor[24] Substitution of the harmonic plane wave $\overline{Q}_{i,j;m}(t) = \widetilde{Q}_m e^{I\left[k\left((iB_{1x}+jB_{2x})\cos\theta+(iB_{1y}+jB_{2y})\sin\theta\right)-\omega t\right]}$ into (14) yields

$$\sum_{n=1}^{2N}\Big[-I\widetilde{\Omega}V'U_{m,n}+M^{0}_{m,n}+M^{-1}_{m,n}e^{-IK\left(B'_{1x}\cos\theta+B'_{1y}\sin\theta\right)}+M^{+1}_{m,n}e^{+IK\left(B'_{1x}\cos\theta+B'_{1y}\sin\theta\right)}$$
$$+N^{-1}_{m,n}e^{-IK\left(B'_{2x}\cos\theta+B'_{2y}\sin\theta\right)}+N^{+1}_{m,n}e^{+IK\left(B'_{2x}\cos\theta+B'_{2y}\sin\theta\right)}\Big]\widetilde{Q}_n=0\,, \tag{15}$$

where K is the nondimensional wave number, and $\widetilde{\Omega}$ is the nondimensional numerical frequency. The numerical dispersion relation can then be written as

$$\Big|-I\widetilde{\Omega}V'\mathbf{U}+\mathbf{M}^{o}+\mathbf{M}^{-1}e^{-IK\left(B'_{1x}\cos\theta+B'_{1y}\sin\theta\right)}+\mathbf{M}^{+1}e^{+IK\left(B'_{1x}\cos\theta+B'_{1y}\sin\theta\right)}$$
$$+\mathbf{N}^{-1}e^{-IK\left(B'_{2x}\cos\theta+B'_{2y}\sin\theta\right)}+\mathbf{N}^{+1}e^{+IK\left(B'_{2x}\cos\theta+B'_{2y}\sin\theta\right)}\Big|=0\,, \tag{16}$$

from which $\widetilde{\Omega}$ can be readily computed. The quantity $-I\widetilde{\Omega}$ is the so-called Fourier footprint $\Re = \Re^{\mathrm{Re}} + I\Re^{\mathrm{Im}}$ of the discretization, $\Re^{\mathrm{Im}}$ being a measure of the dispersive properties of the scheme, and $\Re^{\mathrm{Re}}$ being a measure of the diffusive properties. To ensure stability, $\Re^{\mathrm{Re}}$ should be nonpositive for all K, θ, and ψ.

IV. Partition design and optimization

Families of SV partitions which are considered here, as with those considered in Chen[21] and Van den Abeele and Lacor[24], contain quadrilateral, pentagonal, and hexagonal CVs. It turns out that for an interpolation polynomial of degree m, there must be 3 quadrilateral corner CVs, $3(m\text{-}1)$ pentagonal side CVs, and $(m^2\text{-}3m+2)/2$ hexagonal interior CVs. Initially a uniform partition of this family is generated, as shown in Figure 2 for polynomials of degree 3, 4, and 5.

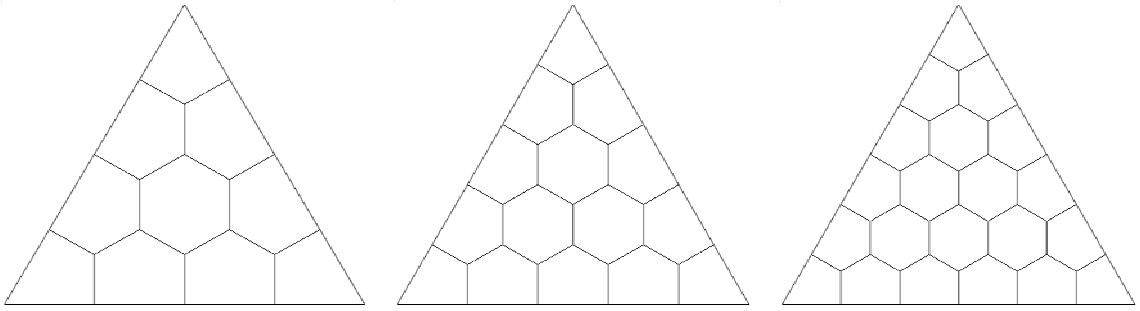

(a) (b) (c)

Figure 2. Uniform partitions for polynomials of degree 3 (a), 4 (b), and 5 (c).

The parameters that uniquely define the SV partition, which will subsequently be referred to as the control vector, can then be determined. The control vector essentially contains the locations of the nodes which physically define the shapes of the CVs within the SV. If any linear manipulation of the SV, while keeping the SV center fixed, causes a given node to coincide with any other node, then any movement of that given node is tied to the movement of the "coincident" nodes. These "coincident" nodes will hereafter be referred to as partner nodes, as shown in Figure 3 for partitions of degree 3 and 4. Denote the components of the control vector as (α_4, β_4, γ_4, δ_4) for a 4th order partition. These components refer to positions of the square, circle, diamond, and delta symbols from Figure 3, respectively.

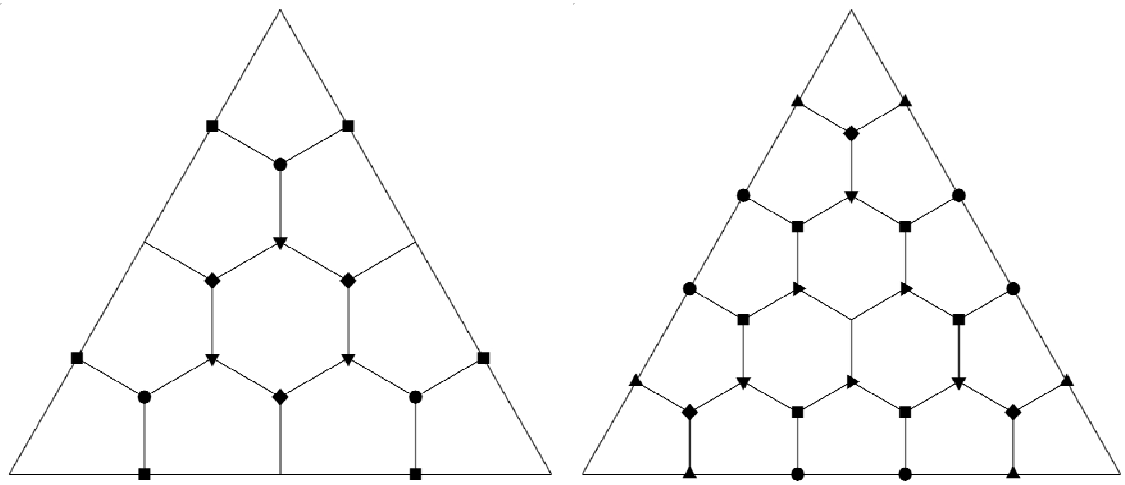

Figure 3. Identification of partner nodes (denoted by like shapes) for partitions of degree 3 (left) and 4 (right). The degree 3 partition is completely defined by 4 parameters, whereas the degree 4 partition requires 7 parameters.

Thus if a given node is found to have partner nodes, for simplicity, the control vector need only contain the position of the given node. Furthermore, the three corner nodes, as well as the SV center node (if it exists) and the SV edge center nodes (if they exist) are omitted from the control vector, since they are immovable. Finally, if a node exists on an SV edge or on an SV line of symmetry, that node is constrained to move along a line and is thus represented by a single coordinate in the control vector, while all other nodes are unconstrained and are represented by two coordinates in the control vector.

The constrained minimization program called CONMIN[29] is employed to optimize the SV partitions. CONMIN is a gradient-based optimizer which utilizes the method of Feasible Directions[30] to find the Feasible Direction, and then move in that direction to update the control vector. The objective or cost function for CONMIN is taken to be the maximum real part of the Fourier footprint of the scheme $\Re_{\max}^{\mathrm{Re}}$. Since CONMIN is used for minimization, it will attempt to drive $\Re_{\max}^{\mathrm{Re}}$ to as low a value as possible, and if it reaches a nonpositive value, a stable partition has been discovered. Then, upon discovery of many stable partitions, those with the lowest dissipation and dispersion are deemed likely to be suitable for simulation.

V. Results

The constrained minimization approach outlined above has been applied to a 4^{th}-order SV partition. In Figure 4, we present a new partition denoted as “SV4H”, and compare with a partition previously proposed by Van den Abeele et al.[24] denoted as “SV4P”, which is known to have favorable stability properties and high accuracy. The control vectors and Lebesgue constants for both the “SV4H” and “SV4P” partitions are given in Table I for comparison. In Figure 5 we present the dispersion and dissipation errors for the both partitions as a function of wave number, leaving the wave angle fixed at $\pi/6$. It is evident that the new partition proposed here has better agreement with the exact solution for a wider range of wave numbers than partition “SV4P”. In addition, plots of the corresponding Fourier footprints in Figure 6 show that the “SV4H” partition also has a smaller Fourier footprint than the “SV4P” partition, and thus will allow for larger time steps to be taken. To validate this analysis numerically, both partitions are used to solve the problem of linear advection of a sine wave on a 10x10x2 grid with periodic boundary conditions. The solution is carried out until time=400. Figure 7 shows the time history of the residual for this simulation, and it is clear that the "SV4H" partition has considerably less damping than the "SV4P" partition. It is thus apparent that the "SV4H" partition is capable of preserving a wave for a longer period of time than the "SV4P" partition on the same grid.

Table I. Control vector and Lebesgue constant for "SV4P" and "SV4H" partitions.

Partition	α_4	β_4	γ_4	δ_4	$\|\|\Gamma_M\|\|$
SV4P	0.07800000	0.07800000	0.03900000	0.26325000	4.2446
SV4H	0.12061033	0.09097092	0.05000000	0.23419571	4.0529

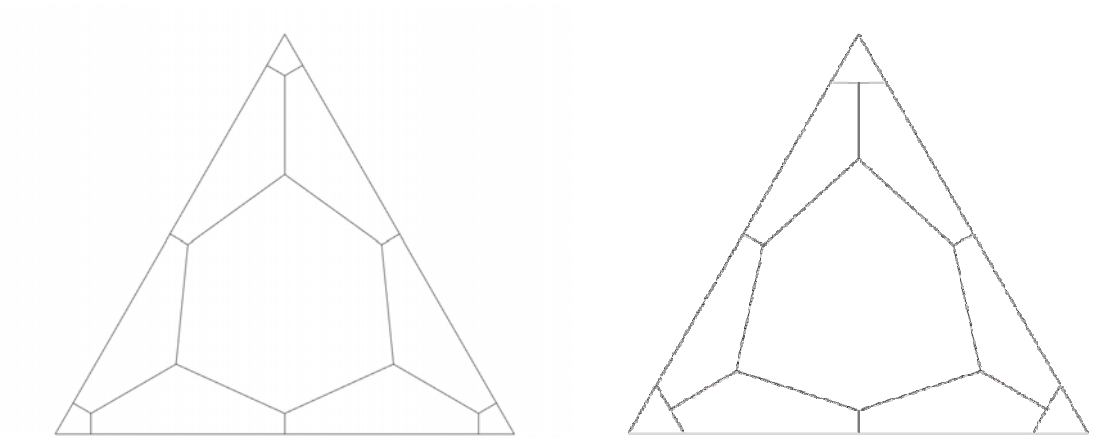

(a) **(b)**

Figure 4. Partitions for 4th-order SV schemes; (a) "SV4P" proposed in Van den Abeele et al.[24]; (b) "SV4H" proposed here.

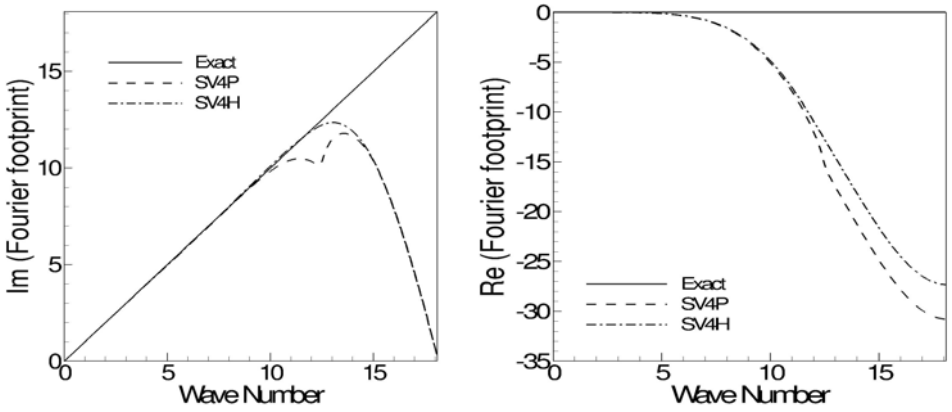

(a) **(b)**

Figure 5. Dissipation and dispersion errors as a function of wave number for various 4th-order partitions. The wave angle considered here is π/6. (a) dispersion error vs. wave number; (b) dissipation error vs. wave number.

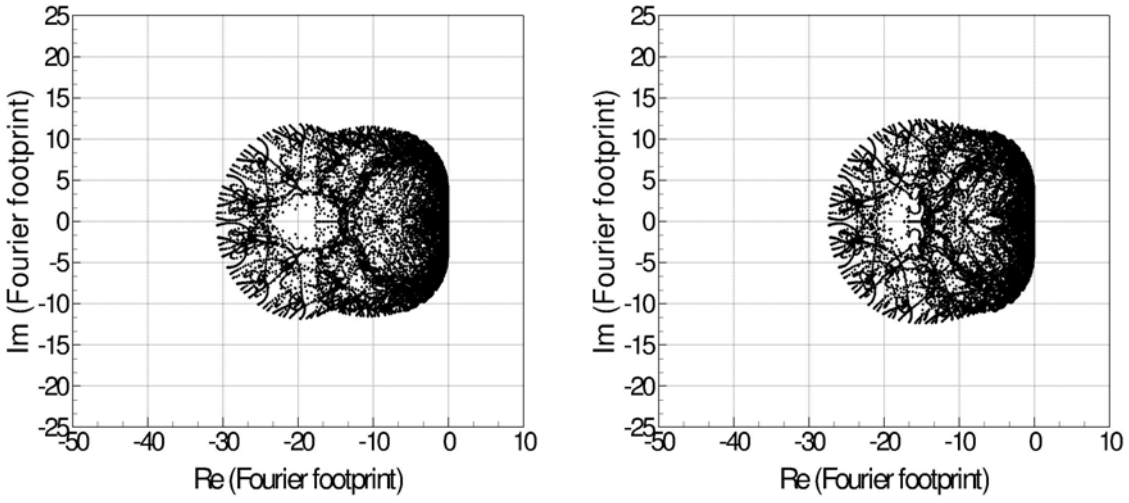

(a) **(b)**

Figure 6. Fourier footprint for 4th-order partitions; (a) "SV4P"; (b) "SV4H".

The new approach has also been applied to a 5th-order partition, and preliminary studies have produced some stable 5th-order partitions. An example of a stable 5th-order partition and its corresponding Fourier footprint are shown in Figure 8. Although more work still needs to be done to minimize the dissipation and dispersion errors of the partition, it is now very promising that this procedure can be used to design stable SV partitions of arbitrary order.

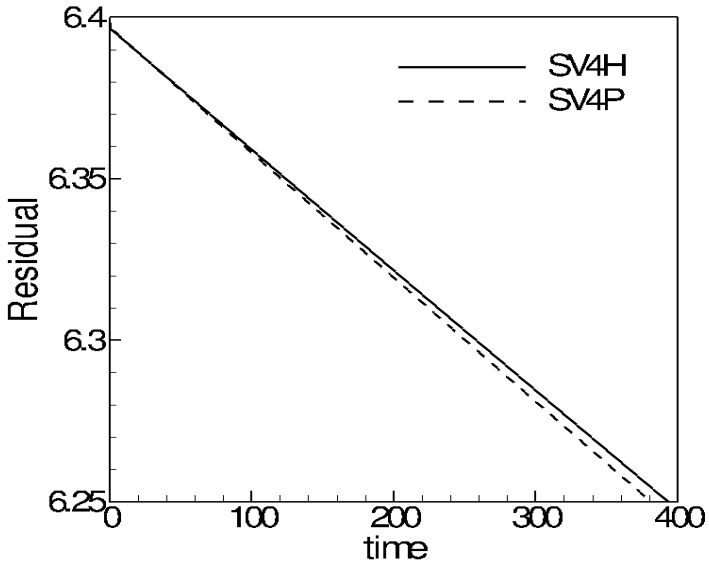

Figure 7. Residual vs. time history for 4th order simulation of the linear advection of a sine wave in a 10x10x2 domain with periodic boundary conditions.

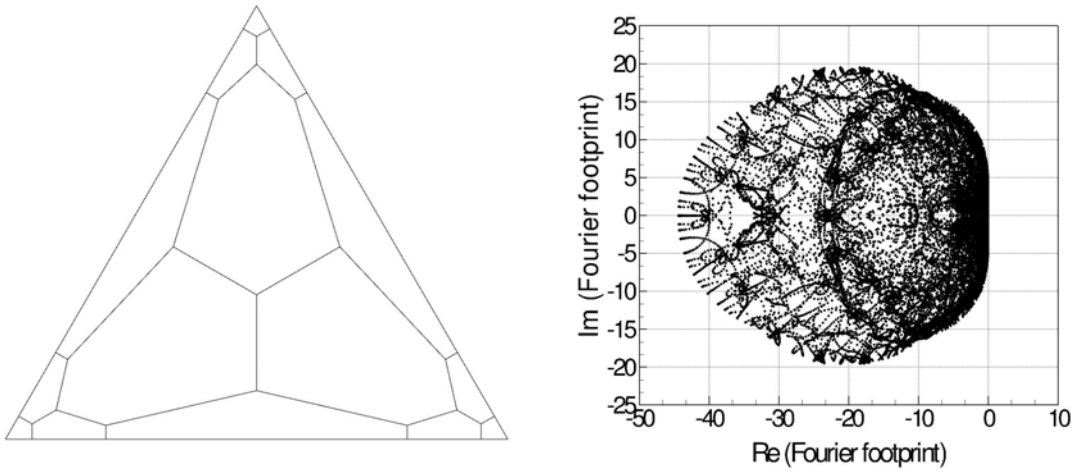

Figure 8. Stable 5th order partition (left) and corresponding Fourier footprint (right).

VI. Conclusions

A new method for obtaining stable SV partitions with low dissipation and dispersion errors via constrained minimization has been presented. The methodology for automatically generating a uniform partition and extracting the parameters that define the design space was outlined. Preliminary results were given for both 4th and 5th order partitions which demonstrate the potential of this method for producing stable and highly accurate partitions of arbitrary order. In particular, a new improved 4th-order partition was presented which posesses superior stability properties and a significant reduction in dissipation and dispersion error over previously used partitions. Additionally, the SV method was extended to 5th-order accuracy and a new stable 5th-order partition is introduced.

Acknowledgements

This study has been supported by the Air Force Office of Scientific Research (AFOSR) and the Department of Energy (DOE) during the doctoral research of the first author while at Iowa State University. The views and conclusions contained herein are those of the authors and should not be interpreted as necessarily representing the official policies or endorsements, either expressed or implied, of the AFOSR and DOE.

References

1. Z. J. Wang, Spectral (finite) volume method for conservation laws on unstructured grids: basic formulation, J. Comput. Phys. 178 (2002) 210.
2. Z. J. Wang, Y. Liu, Spectral (finite) volume method for conservation laws on unstructured grids II: extension to two-dimensional scalar equation, J. Comput. Phys. 179 (2002) 665.
3. Z. J. Wang, Y. Liu, Spectral (finite) volume method for conservation laws on unstructured grids III: extension to one-dimensional systems, J. Sci. Comput. 20 (2004) 137.
4. Z. J. Wang, Y. Liu, Spectral (finite) volume method for conservation laws on unstructured grids IV: extension to two-dimensional Euler equations, J. Comput. Phys. 194 (2004) 716.
5. Y. Liu, M. Vinokur, Z. J. Wang, Spectral (finite) volume method for conservation laws on unstructured grids V: extension to three-dimensional systems, J. Comput. Phys. 212 (2006) 454-472.
6. Y. Sun, Z. J. Wang, Y. Liu, Spectral (finite) volume method for conservation laws on unstructured grids VI: extension to viscous flow, J. Comput. Phys. 215 (2006) 41-58.

7. R. Harris, Z. J. Wang, Y. Liu, Efficient quadrature-free high-order spectral volume method on unstructured grids: Theory and 2D implementation, J. Comput. Phys. 227 (2008) 1620-1642.
8. S. K. Godunov, A finite-difference method for the numerical computation of discontinuous solutions of the equations of fluid dynamics, Mat. Sb. 47 (1959) 271.
9. B. van Leer, Towards the ultimate conservative difference scheme V. a second-order sequel to Godunov's method, J. Comput. Phys. 32 (1979) 101-136.
10. T. J. Barth, P.O. Frederickson, High-order solution of the Euler equations on unstructured grids using quadratic reconstruction, AIAA Paper No. 90-0013, 1990.
11. M. Delanaye, Yen Liu, Quadratic reconstruction finite volume schemes on 3D arbitrary unstructured polyhedral grids, AIAA Paper No. 99-3259-CP, 1999.
12. A. Harten, B. Engquist, S. Osher, S. Chakravarthy, Uniformly high order essentially non-oscillatory schemes III, J. Comput. Phys. 71 (1987) 231.
13. R. Abgrall, On essentially non-oscillatory schemes on unstructured meshes: analysis and implementation, J. Comput. Phys. 114 (1994) 45-58.
14. C. Hu, C.-W. Shu, Weighted essentially non-oscillatory schemes on triangular meshes, J. Comput. Phys. 150 (1999) 97-127.
15. Z.J. Wang, High-Order Methods for the Euler and Navier-Stokes Equations on Unstructured Grids, Journal of Progress in Aerospace Sciences, Vol. 43 No. 1-3 (2007).
16. B. Cockburn, C.-W. Shu, TVB Runge-Kutta local projection discontinuous Galerkin finite element method for conservation laws II: general framework, Math. Comput. 52 (1989) 411-435.
17. B. Cockburn, S.-Y. Lin, C.-W. Shu, TVB Runge-Kutta local projection discontinuous Galerkin finite element method for conservation laws III: one-dimensional systems, J. Comput. Phys. 84 (1989) 90-113.
18. B. Cockburn, S. Hou, C.-W. Shu, TVB Runge-Kutta local projection discontinuous Galerkin finite element method for conservation laws IV: the multidimensional case, Math. Comput. 54 (1990) 545-581.
19. B. Cockburn, C.-W. Shu, The Runge-Kutta discontinuous Galerkin method for conservation laws V: multidimensional systems, J. Comput. Phys. 141 (1998) 199-224.
20. H. L. Atkins, Chi-Wang Shu, Quadrature-free implementation of the discontinuous Galerkin method for hyperbolic equations, AIAA J. 96 (1996) 1683.
21. Q.-Y. Chen, Partitions of a simplex leading to accurate spectral (finite) volume reconstruction. SIAM J. Sci. Comput. Vol. 27, No. 4 (2006) 1458-1470.
22. Q.-Y. Chen, Partitions for spectral (finite) volume reconstruction in the tetrahedron, SIAM J. Sci. Comput. (2005).
23. K. Van den Abeele, T. Broeckhoven, and C. Lacor, Dispersion and Dissipation properties of the 1D spectral volume method and application to a p-multigrid algorithm, J. Comput. Phys. 224 (2) (2007) 616-636.
24. K. Van den Abeele, and C. Lacor, An accuracy and stability study of the 2D spectral volume method, J. Comput. Phys. 226 (1) (2007) 1007-1026.
25. K. Van den Abeele, G. Ghorbaniasl, M. Parsani, and C. Lacor, A stability analysis for the spectral volume method on tetrahedral grids, (submitted to Elsevier Science, 3-17-2008).
26. S. Gottlieb, C-W. Shu, E. Tadmor, Strong stability-preserving high-order time discretization methods, SIAM Review, v.43 n.1, p. 89-112, 2001.
27. R. Harris and Z.J. Wang, High-Order Adaptive Quadrature-Free Spectral Volume Method on Unstructured Grids, AIAA Paper No. 2008-779.
28. R. Harris and Z.J. Wang, High-Order Adaptive Quadrature-Free Spectral Volume Method on Unstructured Grids, Computers and Fluids (under review).
29. N. G. Vanderplaats, CONMIN USER'S MANUAL, Ames Research Center and U.S. Army Air Mobility, R&D Laboratory, Moffet Field, Calif. 94035, 1978.
30. G. Zoutendijk, Methods of Feasible Directions, Elsevier Publishing Co., Amsterdam, 1960.